Small scale hydrogeomorphic features influence macroinvertebrate food webs in two Great Plains rivers

By

Jackob Lutchen

B. FA., University of Minnesota-Morris, 2016

Submitted to the graduate degree program in Ecology and Evolutionary Biology and the Graduate Faculty of the University of Kansas in partial fulfillment of the requirements for the degree of Master of Arts.

_____

Dr. James H. Thorp, Committee Chairman

_____

Dr. Andrew Short

_____

Dr. Frank deNoyelles

Date Defended: May 12th, 2020

The thesis committee for Jackob Lutchen

Certifies that this is the approved version of the following thesis:

Small scale hydrogeomorphic features influence macroinvertebrate food webs in two Great Plains rivers

_____

Chair: Dr. James H. Thorp

Date Approved: May 15th, 2020

Abstract

Food resources that support river food webs and food web structure have been shown to be influenced by hydrogeomorphology, and its influence on food webs has been gaining support with ecologists over the years. I analyzed the influence of local hydrogeomorphic variables on the structure and function of food webs in two U.S. Great Plains rivers, the Little Missouri and Niobrara. I used stable isotope analysis to reveal hydrogeomorphic relationships with $\delta^{13}C$ in the food web, consumer resource use, trophic community metrics and size corrected standard ellipse area (SEAc) a measure of consumer niche breadth. I found river sinuosity and percent fine grain sediment to have a large influence on the food web. Increasing sinuosity was associated with a decrease in the stable isotope composition ($\delta^{13}C$) of the entire food web and trophic diversity ($p=0.038$, $R^2=31.1\%$), but an increase in trophic niche specialization ($p=0.013$, $R^2=41.1\%$). Increasing percent fine sediment was also associated with a decrease in the $\delta^{13}C$ of the food web, as well as higher consumption of autochthonous resources and terrestrial coarse particulate organic matter (CPOM); and a decrease in trophic redundancy (fewer species occupying the same trophic niche). These results suggest that the decrease in stable substrate probably caused an overall decrease in primary productivity and limited autochthonous growth to pools and slackwater areas. This decrease in primary productivity also caused the decrease in overall food web $\delta^{13}C$. The consumption of autochthonous resources and CPOM increased with slow water due to the lack of stable substrate in the majority of the system. Results also indicated that species became more specialized in their trophic niche likely due to decreased diversity. My study gives support to the importance of local hydrogeomorphic variables such as sediment size and sinuosity, on food web structure and trophic interactions in Great Plains rivers. Future studies could expand the number of study rivers in the Great Plains to increase the number and diversity of hydrogeomorphic variables and organisms analyzed.

Acknowledgements

I would like to thank my Advisor Dr. Thorp for his expertise and guidance throughout my time at the University of Kansas and for the opportunity to join the MACRO project where I was able to meet many new people and travel to new places. I would also like to thank my committee members Drs. Andrew Short and Frank DeNoyelles for aiding me in algae identification, providing me with an awesome class on insects and serving on my committee for my masters thesis.

I also would like to thank my fellow lab mates Caleb, Emily, Greg and Karen for their advice and friendship throughout all of my time at KU. I would also like to thank the other members of the bug crew Boloroo, Tsooj, Galaa, Khaliun as well as Bashta and Batra for their aid in the collection of my insect samples. A special shout out to John Tran and Jody Cho for their help in processing all of my stable isotope samples, this project would not have been possible without them. I'd also like to thank John Costello and the others from the South Dakota School of Mines and Technology for collecting the hydrogeomorphology data used in my study. Bruce Barnett also deserves a special thank you for analyzing the 1000+ samples that I sent him.

I also would like to thank NSF for providing funds to make this project and all of the other projects on the MACRO project possible. My research was completed under grant number 0072648 which was awarded to James Thorp, Walter Dodds, Mark Pyron, Alain Maasri, Scott Kenner, Sudeep Chandra, Bazartseren Boldgiv, Mendsaikhan Bud, Dan Rueman, Barbra Hayford, Jon Gelhaus and Olaf Jensen.

Last but not least, I would like to thank my family and friends for all of their love and support throughout my time at KU and especially my wife for her love and patience for me when I stop to look at all of the cool bugs I find.

Table of contents

Introduction

The structure and function of aquatic food webs are influenced by a myriad of biotic and abiotic factors. Among the numerous studies that have analyzed factors potentially influencing food webs, a growing theme has been the effects of hydrogeomorphic characteristics. Hydrogeomorphology is defined as the study of the interactions between hydrologic and geologic processes, landforms or earth materials, and surface to subsurface water in time and space (Poole, 2010). These hydrogeomorphic processes can occur at scales ranging in size from instantaneous stream velocity in a riffle to stream discharge of the watershed. Acting at both large and small scales, hydrogeomorphic processes can have significant effects on the structure and function of aquatic food webs in lotic systems (Thorp et al., 2006; Thoms et al., 2017).

One major interaction of the food web with its environment is the flow of carbon in the system. Carbon flow in food webs can be analyzed using stable isotopes, in particular, the natural variation in the ratio of heavy (^{13}C) to light (^{12}C) isotopes to obtain the carbon signature ($\delta^{13}C$). Carbon isotopes are useful in carbon flow studies because primary producers have distinct isotopic signatures based on their particular photosynthetic pathway, and these signatures change relatively little during conversion from producer tissue to consumer tissue (Gannes et al., 1998). Hydrogeomorphic characteristics have been shown to influence $\delta^{13}C$ of organisms in food webs. As examples, $\delta^{13}C$ signatures of periphyton and sculpin were found to be significantly related to drainage area in three mountain watersheds (Sullivan, 2013), and the ^{13}C of macroinvertebrate consumers increased from mountain sites downstream to hill sites in the main stem of a Japanese river in association with an increased stream width (Kobayashi et al., 2011). Additionally, stream velocity has been shown to influence periphyton and algal $\delta^{13}C$ signatures in forested streams of California and Canada (Finlay, 2004; Rasmussen et al., 2010).

Consumer resource use in rivers has been a popular question for ecologists and has spurned numerous studies and conceptual models. One conceptual model, the River Continuum Concept (RCC), hypothesized that resource use of aquatic communities was largely based on the location along a cline

from headwaters to river's mouth (Vannote et al., 1980). The RCC predicted that an aquatic community's major food source in headwaters is terrestrial coarse particular organic matter (CPOM) as a result of extensive canopy cover that blocks out light for autochthonous production and increased CPOM additions. However, the dominant food source should then change to algae as the stream widens which allows light to reach the bottom. The model further proposed that communities closer to the river's mouth depend on the leakage of food resources from upstream because decreased light penetration from increased water depth and turbidity limit algal productivity (Vannote et al., 1980). While the RCC focuses more on stream width and depth to explain how consumers use resources in a food web, it was developed mainly for rivers in forested catchments and not those in other regions like the Great Plains. A more recent conceptual model challenged this clinal perspective on food webs and focused more on how hydrogeomorphic patterns affect consumer resource use (Thorp et al., 2006). Other studies have also found similar importance in hydrogeomorphic structure, such as a study in Alaskan boreal streams that found that streams with steeper gradients had a higher amount of algae assimilated by caddisfly larvae likely resulting from lower water temperatures and a higher amount of diatom production (Smits et al., 2015).

Community trophic metrics can reveal trophic structure using stable isotopes to compare communities across time and space. Trophic metrics can be determined to analyze multiple, similar food webs across gradients or one food web over time (Layman et al., 2007). These metrics allow us to quantify aspects of community structure, such as trophic diversity and diet similarity in a food web. Some published studies have documented differences in trophic structure after an exotic species introduction or have tracked temporal changes in a food web (Schmidt et al., 2009; Zambrano et al., 2010). However, few studies have analyzed the influence of hydrogeomorphology on community trophic metrics, and no studies have been conducted in grassland ecoregions. As an expansion on the community wide trophic metrics, standard ellipse area (SEA) is a way to analyze niche breadth and overlap of niche breadth in individuals or smaller groups within a community (Jackson et al., 2011). Niche space takes a slightly

different approach from community trophic metrics in that it allows investigators to analyze whether a consumer of interest is a specialist or generalist as well as how its diet overlaps with others in its community (Newsome et al., 2007; Jackson et al., 2011).

Food webs in prairie stream systems have received very little attention even though they are dynamic systems and drain large areas of the USA. Prairie streams are typically fed through storm runoff, which can affect turbidity, and can vary from extremely clear water in the Chikaskia river of Kansas to extremely turbid in the Washita of Oklahoma (Matthews, 1988). Storm run off can also be highly variable with flooding and periods of drought common in prairie rivers. Periods of flooding can disturb biota by flushing them downstream and rearranging the substrate of the stream, affecting recolonization. However, periods of drought could constrain biota to pool refugia due to stream drying. The dynamic nature of prairie rivers makes them a valuable study system for investigating the effects of varying hydrogeomorphology on food webs. Furthermore, understanding those effects could better inform conservation practices in commonly overlooked prairie rivers.

The aim of my study was to measure how hydrogeomorphology affects prairie stream food webs. In particular, I asked the following questions:

- How does hydrogeomorphology influence the $\delta^{13}C$ of macroinvertebrate consumers and their putative resources?
- How does hydrogeomorphology affect the resources used by macroinvertebrates?
- How does hydrogeomorphology influence trophic community metrics and niche breadth of families and functional feeding groups?

To answer these questions, I analyzed $\delta^{13}C$ signatures of major groups of aquatic macroinvertebrates and their putative resources to estimate consumer resource use and food web structure in two Great Plains river systems. These data were then correlated with different local hydrogeomorphic variables to reveal any significant relationships present.

Methods

Study sites

The studied systems were the Little Missouri River and the Niobrara River in the Great Plains ecoregion of the USA. The Little Missouri River begins in northeastern Wyoming and flows through southwestern Montana, northwest South Dakota and western North Dakota before joining the Missouri River (Fig. 1). The substrate of the Little Missouri River was dominated by sand/silt (46.32-75.79%) but contained a small amount of cobble substrate (0-11%), a moderate amount of coarse gravel (3.16-17.89%) and slightly more fine gravel (13.68-30.53%) as shown in Table 1. Riparian vegetation mainly consisted of grasses and shrubs, such as western wheatgrass (*Pascopyrum smithii)* and sandbar willow (*Salix interior*), and sparse coniferous and deciduous trees. Discharge across the Little Missouri sites ranged 0.2-1.03m^3/s (Table 1). The Niobrara River begins in Wyoming and flows through northern Nebraska before joining the Missouri River in the city of Niobrara, NE (Fig. 2). The Niobrara's substrate was composed almost entirely of sand (45.16-93.68%). The discharge ranged between 0.8-33.15 m^3/s.

General site locations were chosen based on the RESonate tool, a GIS-based program that categorizes sampling sites based on large scale hydrogeomorphic and geological characteristics (Williams et al., 2013). The large-scale metrics range from river valley width, mean annual precipitation and elevation, with a total of 13 metrics. However, sites sampled in the field were modified where necessary based on accessibility and land access. Local hydrogeomorphic measurements were collected at each site. Sampling took place between the 7th and 29th of September 2018, and 7 sites were analyzed in each river (Figs. 1-2).

Field collection of macroinvertebrate consumers and resources

Macroinvertebrates were collected qualitatively using a D-net with multiple sweeps of submerged overhanging vegetation as well as direct picking of organisms off rocks and wood when those substrates were present. Pools, runs, cut bank areas and riffles (when present) were all sampled with equal effort. However, the main channel was not sampled extensively because of the lack of stable substrate, unless

favorable habitats were present. Collected organisms were immediately preserved in 80% ethanol until lab processing.

Filamentous algae and macrophytes were collected manually by picking them from various substrates and were then immediately stored in 80% ethanol for later lab processing. Macrophytes were only collected in the Niobrara, while filamentous algae were collected in most sites from both rivers. Epilithic biofilms were scraped with a wire brush and the resulting slurry was frozen. Biofilm was only collected from a few sites due to a lack of stable substrate for biofilm growth. Senesced grasses and leaves (terrestrial coarse particulate organic matter, or CPOM) in the river were collected when available at each site. From here on out CPOM is considered only senesced leaves and grass and a separate food source from detritus.

Laboratory processing of macroinvertebrate consumers and sources

Macroinvertebrates were identified to at least the family level and genus if necessary, in order to constrain the functional feeding group using Merritt et al., (2008) and Thorp et al., (2015). Macroinvertebrate internal organs remained intact as gut clearance has little effect on isotopic signatures (Kaehler et al., 2001; Jardine et al., 2005; Cremona et al., 2009). Filamentous algae were manually picked through to remove inorganic material and macroinvertebrates, but some detritus was impractical to remove completely. Macrophytes were identified to species when possible.

Biofilm slurries were thawed in the lab and separated into algal and detrital fractions using Ludox TM-50 (Hamilton et al., 2005). The Ludox solution was diluted to a concentration of 1.27 g/cm^3 using deionized water and then homogenized. Five ml of biofilm slurry was then pipetted into 30 ml of Ludox solution and centrifuged for 10 min at 1000 rpm. The top algal layer and bottom detrital layer were removed and transferred to separate centrifuge tubes to be concentrated by further centrifugation. This process was repeated until all the biofilm slurry was exhausted. The algal fraction was then pipetted onto

a 47 Whatman mm gf/f filter (pore size 0.7 um) then rinsed to remove the Ludox solution. The detrital fraction had the Ludox solution removed, and DI water was then added to the 40 ml mark before the detrital fraction and water were centrifuged at 1000 rpm for 10 min to remove any remaining Ludox solution from the detrital fraction. This was repeated three times to sufficiently remove the Ludox solution.

All macroinvertebrate and resource samples were rinsed and dried at 60°C for 48 hr, then homogenized to a powder using a Wig-L-Bug mixer or by hand using a mortar and pestle. Macroinvertebrates were ground whole to obtain enough biomass for each sample. Snails were manually removed from their shells and crayfish tail tissue was used to avoid contamination by inorganic C in shell tissue and other exoskeleton tissue (McConnaughey et al., 2008). At least 2-5 individuals of various sizes were homogenized together to obtain a community value for each family (individuals of different sizes). Insects that were at least 6.35 cm (only three large Belostomatidae, giant aquatic bugs) were above this cut off and had a leg removed and homogenized for stable isotope analysis. Legs were removed because they were easier to homogenize in the Wig-L-Bug mixer and did not significantly diminish the value of the insects very much for later deposition in the university museum collection. The detrital fraction material was first measured into silver capsules, and a small amount of water was added to each sliver capsule and acid fumigated for 6-8 hr to remove potential inorganic carbonates. Silver capsules were then re-dried at 60 °C and packed into tin capsules because the tin capsules serve as a catalyst for stable isotope analysis. Homogenized powder of the macroinvertebrate and food resource samples were weighed into tin capsules and sent to the Keck-NSF Paleoenvironmental and Environmental Laboratory at the University of Kansas for analysis. Stable isotope results were reported using the δ notation, where $\delta X = [(R_{sample}/R_{standard}) - 1] * 1000$, with "R" standing for the ratio of heavy to light isotopes. The ratio of heavy to light isotopes of the sample is divided by the ratio of heavy to light isotopes of the standard. The final ratio is multiplied by 1000 to magnify the small differences between the sample and standard (Gannes et al., 1998). Macroinvertebrate and food source samples were analyzed with a ThermoFinnigan Mat 253

isotope ratio mass spectrometer. Precision for $\delta^{13}C$ is 0.2‰ and 0.3‰ for $\delta^{15}N$ based on international standards which are Vienna – Pee Dee Belemnite for carbon and atmospheric air for nitrogen.

Data analysis

I used Bayesian mixing models to quantify dietary contributions of food resources to consumers. Bayesian mixing models take into account the uncertainty that arises from trophic enrichment factors, field collection and variation in consumer isotopic signatures. However, Bayesian mixing models can also provide solutions of dietary contributions to consumers even when logical solutions are highly improbable (i.e. none of the food resources contribute to the consumer's diet). Therefore, as a first step to my Bayesian mixing model analysis, I prevented illogical solutions by simulating and visualizing mixing polygons for each site. (Smith et al., 2013). The mixing polygons take into account the mean and standard deviation of $\delta^{15}N$ and $\delta^{13}C$ of each consumer and dietary resource. The trophic enrichment factor is applied only to dietary resources to account for source specific trophic enrichment (Smith et al., 2013). Mixing polygons were created by iterative re-sampling of isotopic source data from a univariate normal distribution followed by trophic enrichment data, also from a univariate normal distribution. Iterations were run until the variance in the mixing polygon's area stabilized (Smith et al., 2013). The proportion of iterations that demonstrated a logical solution (i.e. inside the mixing polygon) was calculated, which can be interpreted as the frequentist's probability that a logical solution for the consumer can be found. Any consumer that had a proportion of less than 5% of solutions found was excluded from the model because a logical solution with the given dietary sources was unlikely to be found (Smith et al., 2013). An example of a mixing polygon output for an excluded site is in SI Fig 1.

Bayesian mixing models were implemented using mixSIAR (Stock et al., 2018) which accounts for a suite of different errors associated with stable isotope analysis. In this study, multiple consumer and producer samples were pooled together to get enough material for stable isotope analysis. Therefore,

residual error variance was taken into account in model processing because this error term accounts for errors with aggregating multiple individuals (Stock et al., 2018). Generalist priors using the Dirichlet distribution were used in all of the models with an alpha of 1,1,1. Raw isotope data was used in all models and results from analysis were not accepted until no variables were above 1.1 for the Gelman-Rubin diagnostic and no more than 9% above the chains that have not converged using the Geweke diagnostic. If the chains in the Geweke diagnostic were slightly above 5% the Gelman-Rubin diagnostic had 0 chains above 1.1. Given that most of the models had 5 or more potential food sources, those sources were combined *a priori* to give a favorable mixing space (model chains will converge giving a solution) as well as *a posteriori* to reduce the spread of the credible interval for each diet proportion (Stock et al., 2018). Sources were generally combined *a posteriori* to make three distinct source types: autochthonous, CPOM, and detritus to give more constrained credible intervals. Trophic fractionation values of 0.4‰ with a standard deviation of 1.3‰ for $\delta^{13}C$ and 3.4‰ with a standard deviation of 1‰ for $\delta^{15}N$ were used in the mixing models (Post, 2002).

Food resources, must be distinctly different from one another with respect to isotope signatures in order to determine whether a consumer is using a certain resource. If resources are not distinctly different then the Bayesian mixing model cannot differentiate between them and the model output will be inaccurate. Non-distinct resources can be combined to create one distinct resource (Table 3). Resources were only combined if they were biologically similar (*e.g.*, CPOM and filamentous algae were not combined even if they had similar isotope signatures). Differences among stable isotope signatures of unique resources were tested using ANOSIM. The R statistic is robust to small sample sizes. A pairwise result with an $R>0.8$ was required for significance (Bellamy et al., 2017).

In isotope biplot space, $\delta^{13}C$ and $\delta^{15}N$ signatures serve as x and y coordinates respectively, and one can ascertain different aspects of the food web based on consumer position within that space according to six community trophic metrics (Layman et al., 2007). CR stands for carbon range; the larger the value of this metric, the more food sources are used in the food web. NR is nitrogen range; the larger

this metric is, the more trophic levels there are in the food web. Total area, TA, is the total convex hull area occupied by all the individuals in the food web and represents the overall niche space of the community (Layman et al., 2007). CD represents the mean Euclidean distance of each individual to the mean $\delta^{13}C$ and $\delta^{15}N$ values of the whole food web, which represents trophic diversity of the food web. MNND represents the mean Euclidean distance to each species nearest neighbor; the smaller this metric the more redundant and tightly packed the species are in the food web, meaning more trophic redundancy. Finally, SDNND is the standard deviation to the nearest neighbor distance; the lower the value, the more evenly distributed the species are in isotope space (Layman et al., 2007). Community trophic metrics were calculated using the mean centroid value of each group within their respective communities, the preferred method in the SIBER package (Layman et al., 2007; Jackson et al., 2011). Niche breadth using size corrected standard ellipse size (SEAc), due to small sample sizes for each family and FFG, were calculated using the SIBER package. Niche breadth can be used to analyze the individual's trophic niche and diet specialization (generalist or specialist) as an expansion to the community trophic metrics.

Reach level hydrogeomophic data across 141 different variables were collected at each site concurrently with macroinvertebrate and resource collection (Costello et al. *unpublished dataset*). To simplify analysis and focus on an ecologically meaningful framework, only variables directly related to stream structure, substrate and discharge were included. Further, highly correlated (Pearson $r > 0.80$), and therefore redundant, hydrogeomorphic variables were removed from analysis. The remaining variables (Table 3) were analyzed for relationships with community trophic metrics, isotope signatures of consumers and resources, consumer diet proportions and size corrected standard ellipse area (SEAc) Relationships were analyzed using correlation tests between the different hydrogeomorphic variables and the previously mentioned food web variables. Any statistically significant correlation was analyzed further in a simple regression model. Data analysis was carried out in R (R Development Core Team, 2018) and Minitab® (version 19. State College, PA).

Results

$\delta^{13}C$ signatures

A total of 17 different food sources were collected across all study sites. Autochthonous sources categorized as filamentous algae and macrophytes composed the majority of these sources followed by those in CPOM and detritus groups. Leaves, grass and bulrush (CPOM) were fairly consistent across sites in their $\delta^{13}C$ value, typically only ranging between -30 to -26‰, while filamentous algae, an autochthonous source, varied widely with a range of -38‰ to -19‰ (Table 4). A total of 32 different consumers were analyzed from the 14 different sites. The majority of organisms were insects, but three crustacean taxa and one mollusk taxon were analyzed as well (Table 5). Autochthonous sources were collected at all sites except the Little Missouri site LMR4, where no autochthonous sources were found and biofilm separation failed to obtain any autochthonous material (Table 4).

The majority of the food webs $\delta^{13}C$ was correlated with different local hydrogeomorphic variables. Based off the correlation matrix between autochthonous resources and hydrogeomorphic variables (SI Table 2), five relationships were analyzed with simple linear regressions. All but one of these relationships were statistically significant (Fig. 3); only mean discharge was not significant after outliers were excluded, although it was marginally significant ($p=0.062$, $R^2= 11.1\%$). Sinuosity and percent fine gravel had negative relationships with autochthonous $\delta^{13}C$ ($p=0$, $R^2=32.1\%$ and $p=0.013$, $R^2=14.8\%$ respectively). Mean depth was the last significant relationship ($p=0.013$, $R^2=14.0\%$), and it had a positive relationship with autochthonous sources (Fig 3). The $\delta^{13}C$ of CPOM and detrital sources did not have any significant relationships with any of the hydrogeomorphic variables (SI Table 3). Based on correlations between the $\delta^{13}C$ of the caddisfly Hydropsychidae, predators, scrapers (excluding Niobrara sites NIO7 and NIO2), filterers and hydrogeomorphic characteristics (SI Table 2), these groups tracked most of the same relationships that autochthonous sources had with hydrogeomorphic variables (Figs. 4-7). Sinuosity is a hydrogeomorphic character that had a negative relationship with all $\delta^{13}C$ signatures of

each consumer group, although sinuosity also had the strongest predictive relationship. Mean discharge had a positive relationship with all groups, although in scrapers the relationship lost its significance once the outliers were removed (Fig. 7). Percent fine gravel had a negative relationship with $\delta^{13}C$ for all consumers except for scrapers. Lastly, mean depth had a significant positive relationship with $\delta^{13}C$ of filterers, predators and autochthonous sources (Figs. 4-7).

Mixing models

Bayesian mixing models resolved at nine out of 14 sites. Based on the mixing polygon models, three sites from the Little Missouri: LMR1, LMR2, LMR3 and one site from the Niobrara, NIO2, had to be excluded from subsequent mixing model analysis because none of the consumers fit inside the mixing space (probability of a real solution <5%) or not enough resources were found at that particular site to run a mixing polygon model (e.g., NIO2;SI Fig. 1). Furthermore, Monte Carlo iteration chains did not converge when run at 12 million iterations for site NIO1, so that site was also excluded from subsequent analysis. All other sites showed at least half (NIO7) or more of the consumers as successfully falling within the mixing space. Taxa excluded from the mixing models are listed in SI Table 1. Two sites appeared to return erroneous results after Bayesian mixing models: LMR7 and NIO3. Both models underestimated the contribution of the detrital fraction of biofilm to the diet of multiple consumers (SI Figs. 4-5). Both sites also had very large confidence intervals for the diet proportions so they were left out of analysis with the hydrogeomorphic variables. Therefore, only seven sites: LMR4, LMR5, LMR6, NIO5, NIO6, NIO7 and NIO8 were included in subsequent analyses.

The autochthonous diet proportion of consumers from two sites in the Little Missouri (LMR5 and LMR6) and four sites in the Niobrara (NIO5, NIO6, NIO7 and NIO8) were significantly correlated with six hydrogeomorphic variables (SI Table 5). Percent fine grain sediment, coarse grain sediment and percent pools and glides were all positively correlated *i.e.*, as these variables rose in value the

autochthonous diet proportion of consumers also increased (Fig. 8). However, these relationships were only weakly predictive with R^2 ranging from 10.3 to 19.2%. Finally, discharge did not have a significant relationship with autochthonous diet proportion after the outliers from site NIO8 were removed. The discharge from site NIO8 was 33.15 m^3/s which was by far the highest discharge, and was excluded.

Significant correlations between terrestrial coarse particulate organic matter (CPOM) resource use and hydrogeomorphic variables were observed at three sites in the Little Missouri River: LMR4, LMR5, and LMR6 as well as four sites in the Niobrara: NIO5, NIO6, NIO7, NIO8 (SI Table 5). Percent fine grain sediment and percent pools and glides all increased positively with CPOM consumption (Fig. 9). Discharge and mean slope lost their significance after outliers (site NIO8 for discharge and sites LMR4 and LMR5 for mean slope) were excluded from analysis. There were two significant correlations between hydrogeomorphic variables and the detrital diet proportion of consumers at the sites: NIO6, NIO7, NIO8 in the Niobrara and LMR6 and LMR4 in the Little Missouri River (SI Table 5). The relationships were both negative, the first was between detrital consumer use and sinuosity and the second between percent coarse sediment and detrital resource use (Fig. 10).

Community trophic metrics and niche breadth

The carbon range, a measure of the diversity of food resources, varied between 1.27-6.48 across all sites and the nitrogen range, a measure of the number of trophic levels in the food web, had a range of 2.4-11.4 (Table 6). Total area was highest at NIO1, but other metrics remained relatively consistent throughout the rest of the sites. There were five significant correlations between community metrics and hydrogeomorphic variables (SI Fig. 4). Carbon range increased as mean thalweg depth increased (Fig. 11), and mean distance to the centroid, or trophic diversity, decreased as sinuosity increased (Fig. 12). Both percent coarse and fine grain sediment increased in concurrence with mean nearest neighbor

distance (Fig. 13). Finally, standard deviation of nearest neighbor distance decreased as sinuosity increased, so species were more evenly spaced as sinuosity increased (Fig. 14).

Sample size corrected standard ellipse area (SEAc) for families was typically very small, usually less than 1 (SI Table 3). Invertebrates from the family Belostomatidae had the largest SEAc at sites LMR7 and NIO2 where there were very large individuals included in analysis. However, the SEAc was typically larger when individuals were grouped into FFGs rather than families (SI Table 4). Predators and filterers were the only two FFGs found at all of the sites and predators typically had the largest SEAc area, although gatherers had the largest area at site NIO3 (SI Table 4). There was only one significant correlation between the hydrogeomorphic variables and the SEAc of families and FFGs, percent coarse sediment (SI Figs. 5-6). However, when removing the outliers present in each relationship (the large SEAc area from the giant aquatic insects and predator FFG), they both lose their significance ($p=0.857$ for families and $p=0.574$ for FFG).

Discussion

Numerous studies have demonstrated an influence of local stream hydrogeomorphology on aquatic food webs (Finlay, 2004; Ishikawa et al., 2012; Sullivan, 2013). My study investigated the relationships between local hydrogeomorphology and the $\delta^{13}C$ isotope signatures of the macroinvertebrate food web, consumer resource use, niche width, and community trophic metrics. The results indicate that local hydrogeomorphic characteristics do affect aquatic food webs, although to a variable extent. Local hydrogeomorphic variables were correlated with the decrease in the $\delta^{13}C$ of the food web, but some characters were also correlated with an increase in the $\delta^{13}C$ of some groups of organisms. Consumer resource use was generally positively correlated with hydrogeomorphology, but detrital resource use was negatively correlated. Niche breadth of families and FFGs were not correlated with any hydrogeomorphic variables. Carbon range was positively correlated with hydrogeomorphology along with trophic specialization, but trophic diversity was negatively correlated with hydrogeomorphology.

$\delta^{13}C$ signatures

Hydrogeomorphic characteristics had the strongest predictive relationships with Carbon signatures of food web consumers and resources, with numerous local variables affecting them. The local variables that influenced the food web were related to physical stream characteristics such as sinuosity, mean thalweg depth, and percent coarse or fine grain substrate. The $\delta^{13}C$ of CPOM and detritus did not have significant relationships with any of the hydrogeomorphic variables. The lack of a relationship between the $\delta^{13}C$ of CPOM and detritus could be in part due to the consistent variation in the carbon signature range of terrestrial C_3 plant material and detrital material only being found at nine sites (Ishikawa et al., 2012). The percentage of fine grain sediment and coarse sediment was associated with a decreased carbon signature of autochthonous sources which could be explained by the lack of stable substrate for autochthonous growth. A decrease in growth of autochthonous producers could lead to an overall decrease in primary production, which has been shown to increase the discrimination against $^{13}CO_2$, further decreasing the $\delta^{13}C$ of resources in the food web (Ishikawa et al., 2012). Stream sinuosity may increase the amount of fine sediment suspended within the water column, as a result of the erosion and deposition of stream banks that occurs as the stream meanders and creates point banks. Those hydrogeomorphic processes could explain why there was a decrease of $\delta^{13}C$ in autochthonous resources with increasing sinuosity. Both mean discharge and thalweg depth were positively correlated with the $\delta^{13}C$ of autochthonous sources. Discharge and depth were related to each other because discharge is the product of stream depth, width and velocity. Therefore, those two hydrogeomorphic variables are related to stream size and as stream size increases so does $\delta^{13}C$ (Ishikawa et al., 2012; Sullivan, 2013).

Consumers tracked the relationships autochthonous resources had with local hydrogeomorphic variables, although with some variation. Scrapers only correlation with hydrogeomorphology was with sinuosity and filterers with predators were the only groups positively correlated with thalweg depth. The tracking of autochthonous resources and macroinvertebrate $\delta^{13}C$ signatures was previously reported in the

main stem of a river in Japan (Kobayashi et al., 2011), but here it is reported in Great Plains rivers for the first time.

Mixing models

The increased percentage of fine sediment and percentage of pools was correlated with the increased diet proportion of autochthonous material and CPOM. This could be due to the fact that a lot of food resource sample collection happened in slack water or slow-moving water areas. These areas did not have as much sediment turnover and movement due to low flow, which could allow for sediment stability and potential for autochthonous growth and for CPOM accumulation (Atkinson et al., 2008). Some collected macrophytes are also well adapted for slower moving water, and they were a component of the autochthonous resources that increased with the percentage of pools and fine sediment (Allan et al., 2007). In contrast, the amount of detritus in consumer diets decreased with increased sinuosity and coarse sediment. This is most likely a result of the correlation of increased coarse sediment and autochthonous resource consumption. The only hydrogeomorphic variable showing a negative relationship with autochthonous resource consumption was mean slope. The decrease was largely driven by the Niobrara site NIO8, while the other sites still had a large majority of consumers who had a larger proportion of autochthonous material in their diet.

Community metrics and niche breadth

Carbon source diversity increased with thalweg depth, because of the inherent relationship between stream depth, discharge, and stream width. As stream area increased the amount of light that can penetrate to the bottom of the stream rose, thereby permitting more autochthonous growth. Higher autochthonous production leads to more diversity in food resources available to consumers, leading to a potential increase in carbon range. Mean distance to the centroid (CD) a measure of trophic diversity, decreased as sinuosity increased. This result may be driven by the increase in fine grain sediment associated with sinuosity. Typically as fine sediment increases, the biomass and diversity of macroinvertebrates decrease

due to lack of habitat heterogeneity (Allan et al., 2007). Because the lack of diversity leads to a decrease in trophic interactions and functional feeding groups, trophic diversity decreases as a result. Furthermore, Standard Deviation of Mean Nearest Neighbor Distance (SDNND) decreases with the increase in sinuosity. The decrease in SDNND is an indication that species are more evenly spaced in trophic space, suggesting an even spread of trophic niches. Mean Nearest Neighbor Distance (MNND) showed a direct relationship with the presence of coarse (64-16mm) and fine (sediment size 16-2mm) sediment. Since MNND is related to SDNND it is not surprising that sediment size was related to species spacing in trophic space. Species that are further apart and are not as tightly packed in the food web have more specialized trophic niches. The substrate in the middle of the stream was extremely unstable and most of my sampling occurred in pools and slackwater areas and from picking organisms off woody debris. It is possible that the increase in trophic specialization is due to the presence of few microhabitats within the overall sandy river which, leads to an overall decrease in diversity and occupied trophic niches. In addition, the consumers that I did collect from each site could have been collected from different microhabitats such as woody debris and/or a pool which would further increase trophic specialization. The consumers would use different food resources from each microhabitat and occupy different areas of the food web. Finally, the size corrected standard ellipse area (SEAc) of families and functional feeding groups were not correlated with any hydrogeomorphic variables. Niche breadth of groups in the food web were not affected by hydrogeomorphic variables; it seems that patterns emerge only when groups are analyzed on the community level rather than individual group level. Perhaps at a smaller or more temporal scale we would have seen a pattern emerge.

Synthesis

Hydrogeomorphic variables affected food webs in the two Great Plains Rivers I studied. In particular, $\delta^{13}C$ of the entire food web was influenced by sinuosity and percent fine grain sediment, thereby leading to a decrease in $\delta^{13}C$ of all consumers and autochthonous food resources. These findings are important for Great Plains streams because a large number of them tend to have sandy or clay as the

primary substrate (Matthews, 1988). However, mean discharge and thalweg depth influenced only the $\delta^{13}C$ of: predators, the caddisfly Hydropsychidae and filterers. These data lend support to other studies that found different hydrogeomorphic variables to influence the $\delta^{13}C$ of the food web (Finlay, 2004; Ishikawa et al., 2012; Sullivan, 2013). Discharge and depth can vary throughout the year in Great Plains rivers because of the unpredictability in flow (Matthews, 1988; Dodds et al., 2004). Rivers in the Great Plains are mainly fed by storm run off so there could be a large spate that removes the biota entirely and changes the algal biomass of the system, which in turn, would influence the $\delta^{13}C$ of autochthonous sources and the food web. Periods of low flow could also decrease the $\delta^{13}C$ of the system because of a decrease in primary production.

Consumer resource consumption was also affected by hydrogeomorphology with an increasing amount of CPOM and autochthonous resources used by consumers in slow moving water. In the Little Missouri and Niobrara Rivers, stable substrate is scarce, so pools and slack water habitats provide areas where sediment is stabilized thereby allowing increased autochthonous production and CPOM accumulation (Atkinson et al., 2008). Pools could also serve as refugia for biota during times of low flow and consumers can take advantage of the food resources stored there. However, the contribution of detritus used by consumers fell because CPOM and autochthonous consumption rose in slow moving waters. The influence of hydrogeomorphology on consumer resource consumption lends support to the Riverine Ecosystem Synthesis, a conceptual model which considers hydrogeomorphic influences to be a more important driver of food web function than stream order (Thorp et al., 2006).

Community trophic metrics were affected by sinuosity, with the decrease in trophic diversity and increase in trophic evenness correlated with sinuosity. The rise in fine and slightly larger coarse sediment (which is affected by sinuosity) was correlated to increased trophic specialization within the food web. High amounts of small sediment could diminish macroinvertebrate diversity while decreased diversity in turn could lower the number of trophic niches occupied in the food web. The increase in mean thalweg depth increased the carbon range, or diversity of food resources in the food web. Since mean thalweg

depth is related to stream width and size it further supports studies that found larger systems support more primary production (Ishikawa et al., 2012; Sullivan, 2013). Future studies to expand on my work could include the collection of more families to expand the diversity of organisms analyzed, thereby improving the performance of the Bayesian mixing model from the collection of more food resources. Even further, additional Great Plains rivers could be analyzed to obtain more diverse hydrogeomorphic conditions.

Tables

Table 1. Descriptive hydrogeomorphic information for all sites in the Little Missouri River. The table describes the site code of each location sampled in the Little Missouri as well as: the latitude and longitude, elevation, date sampled and the river sampled from. Variable codes are as follows: XDEPTH; mean thalweg depth (m), PCT_SLOW; glides and pools (%), SINU; channel sinuosity, XSLOPE; water surface gradient over reach (slope), SUB_X; substrate mean size class, PCT_CB; % cobble (250-64mm), PCT_GC; % coarse sediment (64-16mm), PCT_GF; % fine sediment (16-2mm), PCT_SAFN; % sand (2>mm), XDSCHRG; mean discharge (m^3/s).

Descriptive Site Code	LMR1	LMR2	LMR3	LMR4	LMR5	LMR6	LMR7
River	Little Missouri	Little Missouri	Little Missouri	Little Missouri	Little Missouri	Little Missouri	Little Missouri
GPS lat (N)	48.90874	46.32776	46.94951	47.95121	45.43254	45.5486	54.77547
GPS lon (W)	-90.532	-103.918	-103.534	-103.332	-104.054	-103.970	-103.887
Elevation	670	688	682	642	807	786	420
XDEPTH	0.40	0.48	0.40	0.41	0.75	0.71	0.53
PCT_SLOW	90.11%	92.31%	86.81%	83.52%	92.31%	100.00%	86.81%
SINU	2.35	2.34	1.27	1.35	2.74	2.14	2.44
XSLOPE	0.0005	0.0005	0.0003	0.0004	0.0004	0.0008	0.0009
SUB_X	10.60	42.07	21.26	4.94	7.21	8.05	25.28
PCT_CB	2.11%	11.58%	5.26%	0.00%	0.00%	2.11%	6.32%
PCT_GC	12.63%	17.89%	14.74%	3.16%	8.42%	8.42%	15.79%
PCT_GF	24.21%	17.89%	30.53%	23.16%	18.95%	13.68%	18.95%
PCT_SAFN	61.05%	46.32%	48.42%	73.68%	72.63%	75.79%	55.79%
XDSCHRG	0.71	0.53	0.78	1.03	0.08	0.20	0.35

Table 2. Descriptive hydrogeomorphic information for all sites in the Niobrara River. The site code of each location sampled in the Niobrara as well as: the latitude and longitude, elevation, date sampled and the river sampled from. Variable codes are as follows: XDEPTH; mean thalweg depth (m), PCT_SLOW; glides and pools (%), SINU; channel sinuosity, XSLOPE; water surface gradient over reach (slope), SUB_X; substrate mean size class, PCT_CB; % cobble (250-64mm), PCT_GC; % coarse sediment (64-16mm), PCT_GF; % fine sediment (16-2mm), PCT_SAFN; % sand (2>mm), XDSCHRG; mean discharge (m^3/s).

Descriptive Site Code	NIO1	NIO2	NIO3	NIO5	NIO6	NIO7	NIO8
River	Niobrara	Niobrara	Niobrara	Niobrara	Niobrara	Niobrara	Niobrara
GPS lat (N)	42.890212	42.54335	42.78575	42.78909	42.92458	42.54747	42.77076
GPS lon (W)	-100.313	-99.777	-99.709	-100.065	-100.749	-100.104	-98.444
Elevation	979	944	864	685	814	686	590
XDEPTH	0.78	0.72	0.70	0.98	0.55	0.57	0.94
PCT_SLOW	93.41%	19.78%	15.38%	100.00%	69.23%	34.07%	30.77%
SINU	1.19	1.22	1.64	1.07	2.31	1.74	1.03
XSLOPE	0.0013	0.0050	0.0084	0.0010	0.0010	0.0008	0.0011
SUB_X	37.90	20.18	17.92	7.36	3.56	70.34	20.02
PCT_CB	0.00%	3.23%	1.05%	1.05%	1.05%	0.00%	2.11%
PCT_GC	7.45%	30.11%	24.21%	2.11%	1.05%	5.26%	1.05%
PCT_GF	13.83%	19.35%	13.68%	2.11%	3.16%	8.42%	1.05%
PCT_SAFN	65.96%	45.16%	58.95%	93.68%	93.68%	64.21%	83.16%
XDSCHRG	16.79	2.52	1.48	0.77	0.80	1.05	33.15

Table 3. Hydrogeomorphic character codes and their descriptions. Only the non-correlated hydrogeomorphic variable codes and descriptions are included**.**

Variable code	Variable Description
XDEPTH	Mean thalweg depth (m)
PCT_SLOW	Glides and pools (%)
SINU	Channel sinuosity
XSLOPE	Water surface gradient over reach (%)
SUB_X	Substrate mean size class
PCT_CB	% cobble (250-64mm)
PCT_GC	% coarse gravel (64-16mm)
PCT_GF	% fine gravel (16-2mm)
XDSCHRG	Mean discharge (m^3/s)

Table 4. Mean (± one SD) $\delta^{13}C$ and $\delta^{15}N$ signatures of all food the resources across all sites in each river. Isotope signatures were not corrected for trophic enrichment and one standard deviation around the mean is included. Sources with an (*) were combined with another source a priori, sources with a (+) were excluded to make a better mixing space or a mixing model at that site was unable to be run. Resources were grouped into three kinds of resources: autochthonous, CPOM and detritus. Sample size is indicated in the n column.

Source	Resource Type	n	Site	$\delta^{13}C$	$\delta^{15}N$
+Algal fraction	Autochthonous	2	+LMR2	-26.08±0.002	0.5±0.11
		6	LMR6	-29.92±2.19	1.11±1.34
		3	LMR7	-27.24±0.03	0.17±0.42
		3	NIO5	-22.64±0.53	1.33±0.25
		3	+NIO6	-26.14±2.04	2.63±0.64
Bulrush	CPOM	5	LMR7	-27.8±0.31	2.88±0.24
*Coontail	Autochthonous	5	*NIO1	-19.55±0.04	4.82±0.03
		5	NIO5	-19.58±0.12	-8.31±0.31
		5	NIO6	-25.12±0.06	-1.61±0.09
Crowfoot	Autochthonous	5	NIO3	-25.38±0.15	0.99±0.13
CPOM	CPOM	8	NIO5	-28.05±0.09	-0.22±0.11
Decaying algae	Autochthonous	4	LMR5	-32.36±0.28	2.97±0.28
*Detrital fraction	Detritus	3	+LMR2	-26.89±0.09	0.28±0.02
		3	*LMR4	-25.46±0.17	2.58±0.28
		3	*	-26.47±0.05	4.60±0.11
		3	LMR7	-29.71±0.02	0.06±0.06
		3	NIO1	-17.86±0.17	2.45±0.03
		3	NIO3	-27.71±0.06	1.83±0.1
		3	*NIO6	-25.78±0.26	3.59±0.07
		3		-23.47±0.06	2.64±0.11
		3	NIO7	-25.54±0.14	1.61±0.1
		2	NIO8	-24.69±0.03	3.5±0.22
+Detritus	Detritus	4	+LMR2	-24.58±0.67	-0.53±0.05
		4	LMR4	-25.95±0.05	-2.06±0.16
		4	LMR6	-22.77±0.26	2.59±0.15
		4	NIO8	-26.6±0.31	0.98±0.1
Duckweed	Autochthonous	5	NIO5	-28.81±0.12	3.55±0.04
		5	NIO7	-30.51±0.06	0.03±0.19
*+Elodea	Autochthonous	5	*NIO1	-21.27±0.45	4.11±0.11
		5	+NIO3	-29.45±0.5	2.19±0.24
		3		-24.51±0.01	0.18±0.15
		5	NIO6	-27.37±0.16	2.38±0.14
		5	+NIO7	-27.03±0.34	9.7±0.19
Epixyle algae	Autochthonous	4	NIO8	-20.03±0.73	3.57±0.07

*+Filamentous algae	Autochthonous	5	+LMR1	-30.35±0.06	4.65±0.15
		6	+LMR3	-31.65±0.04	5±0.21
		6	+	-32.55±0.16	4.21±0.1
		5	LMR5	-36.18±0.06	0.15±0.14
		5	*LMR6	-33.54±0.17	7.1±0.08
		3	*	-34.21±0.13	7.34±0.03
		4	*LMR7	-34.87±0.19	0.91±0.02
		5	*	-33.56±0.18	1.85±0.2
		5	*	-33.9±0.09	-0.06±0.08
		5	*NIO1	-19.89±0.18	2.56±0.32
		5	*	-19.98±0.14	0.45±0.08
		3	*	-26.47±0.09	3.21±0.03
		5	+NIO2	-22.28±0.04	2.72±0.04
		10	+NIO3	-38.11±0.21	-0.98±0.1
		5		-34.67±0.07	0.12±0.03
		5	*NIO5	-24.12±0.23	2.1±0.23
		5	*	-25.45±0.62	3.08±0.24
		5		-19.38±0.17	2.16±0.15
		5	NIO6	-26.11±0.14	-1.64±0.05
		5	NIO7	-28.54±0.05	1.38±0.1
		2	NIO8	-23.34±0.2	-0.37±0.23
*Grass	CPOM	5	+LMR1	-27.89±0.19	3.84±0.24
		4	+LMR3	-28.40±0.17	2.79±0.16
		5	LMR4	-26.45±0.5	2.17±0.26
		5	*LMR5	-27.19±0.43	2.89±0.06
		5	LMR6	-19.5±0.48	1.10±0.21
		5	NIO1	-27.57±0.19	3.0±0.28
		5	NIO2	-27.53±0.05	4.65±0.11
		5	NIO3	-29.75±0.3	2.85±0.29
		5	NIO6	-26.3±0.32	3.29±0.37
		5	NIO7	-16.04±0.57	1.89±0.23
		5	NIO8	-27.49±0.39	2.92±0.32
+Hedge grass	Autochthonous	5	+LMR2	-17.02±0.07	3.89±0.13
*Leaf	CPOM	5	LMR4	-26.89±0.344	-2.37±0.25
		5	*LMR5	-26.16±0.06	2.35±0.28
		5	LMR6	-28.36±0.38	2.35±0.3
		6	LMR7	-27.92±0.25	-2.05±0.26
		5	NIO1	-28.29±0.25	-0.68±0.14
		6	NIO6	-30.29±0.22	6.86±0.31
		5	NIO7	-27.32±0.26	0.77±0.18

Light fraction	Autochthonous	5	NIO7	-26.4±0.35	-0.14±0.2
Watercrow	Autochthonous	5	*NIO1	-18.99±0.07	1.75±0.1

Table 5. Mean (± one SD) $\delta^{13}C$ and $\delta^{15}N$ isotope signatures of all consumers across all sites. Isotope values displayed are not corrected for trophic enrichment. General information about each consumer is included in different columns as well as the sample size. Baetidae did not have a SD calculated because only one sample of tissue from Baetidae was analyzed.

Family	Organism Type	FFG	n	Site Code	$\delta^{13}C$	$\delta^{15}N$
Athericidae	Insect	Predator	5	NIO2	-23.8±0.16	6.77±0.35
			5	NIO7	-27.00±0.20	4.08±0.30
Baetidae	Insect	Collector Gatherer	1	LMR3	-25.77	3.04
			3	LMR6	-26.72±1.61	1.35±0.13
			5	LMR7	-30.49±.03	0.85±0.06
			5	NIO1	-23.64±0.05	2.25±0.03
			5	NIO3	-25.80±0.06	1.36±0.80
			5	NIO5	-23.11±0.06	3.65±0.11
			5	NIO6	-25.89±0.06	3.28±0.07
Belostomatidae	Insect	Predator	5	LMR3	-26.81±0.50	7.98±2.56
			5	LMR7	-28.56±1.31	6.35±4.11
			10	NIO1	-29.09±0.38	2.81±0.39
			10	NIO2	-28.60±1.22	4.07±2.09
			5	NIO3	-28.94±.020	3.58±0.31
			5	NIO5	-28.39±0.12	2.39±0.16
			9	NIO6	-29.79±0.94	3.14±0.48
			5	NIO7	-29.78±0.31	3.47±0.55
Brachycentridae (brachycentrus)	Insect	Filterer	5	NIO1	-24.34±0.18	3.04±3.04
			5	NIO5	-23.55±0.12	3.31±0.02
			5	NIO6	-26.14±0.32	3.47±0.26
			5	NIO7	-27.12±0.35	1.47±0.24
Calopterygidae	Insect	Predator	5	LMR6	-30.57±0.04	3.51±0.10
			5	LMR7	-29.12±0.15	3.14±1.31
			5	NIO1	-23.75±0.10	4.60±0.11
			5	NIO2	-23.49±0.09	6.60±0.18
			5	NIO5	-23.29±0.27	5.24±0.29
			5	NIO6	-25.37±0.04	4.17±0.16
			5	NIO7	-27.54±0.18	3.76±0.16
			5	NIO8	-22.88±0.16	6.64±0.12
Chironomidae	Insect	Collector Gatherer	5	LMR5	-32.07±0.089	4.41±0.05
			5	NIO3	-27.55±0.29	5.18±0.45
Coenagrionidae	Insect	Predator	5	LMR2	-27.12±0.24	2.58±0.06
			5	LMR4	-26.64±0.10	4.94±0.10
			6	LMR5	-29.79±0.20	4.59±0.19

			5	LMR6	-30.29±0.26	4.74±0.03
			5	LMR7	-30.37±0.04	3.56±0.05
			5	NIO3	-25.25±0.26	5.31±0.10
Cordulidae	Insect	Predator	5	NIO5	-24.38±0.03	3.22±0.09
Corixidae	Insect	Herbivore	5	LMR4	-31.95±0.13	5.97±0.21
			5	LMR5	-30.06±0.25	4.07±0.08
			5	NIO6	-27.10±0.16	2.64±0.18
Corydalidae	Insect	Predator	5	NIO8	-24.02±0.07	6.44±0.14
Dryopidae (Adults)	Insect	scraper	5	LMR2	-24.25±0.11	1.64±0.15
Dytiscidae (Adults)	Insect	Predator	5	NIO3	-27.23±0.15	4.53±0.23
Gerridae	Insect	Predator	5	NIO1	-24.49±0.39	5.40±0.24
Gomphidae	Insect	Predator	5	LMR1	-26.26±0.23	1.90±0.39
			5	LMR4	-28.25±0.11	2.71±0.22
			5	NIO6	-26.71±0.09	4.42±0.13
			5	NIO7	-26.25±0.29	3.88±0.29
Gyrinidae	Insect	Predator	5	NIO1	-27.68±0.10	5.24±0.55
Heptageneiidae	Insect	Scraper	3	LMR1	-26.30±0.03	2.06±0.09
			5	LMR2	-25.43±0.02	1.09±0.07
			5	LMR3	-27.19±0.04	2.13±0.08
			5	LMR4	-25.70±0.06	2.89±0.13
			5	LMR6	-29.67±0.19	-0.11±0.52
			5	LMR7	-29.86±0.12	0.68±0.11
			5	NIO1	-25.59±0.11	2.73±0.17
			5	NIO6	-26.38±0.13	3.78±0.05
			5	NIO8	-24.82±0.02	5.24±0.08
Hydrophilidae (Hydrophilinae)	Insect	Collector Gatherer	5	NIO3	-31.82±0.23	3.65±0.76
			5	NIO5	-33.48±0.64	2.24±0.18
			5	NIO6	-30.51±0.44	5.09±0.32
Hyalella (Hylella)	Crustacean	Shredder	5	LMR7	-29.04±0.27	1.07±0.28
			5	NIO1	-24.50±0.09	2.72±0.15
			5	NIO3	-24.67±0.38	6.40±0.34
			5	NIO5	-22.05±0.072	3.44±0.19
Hydropsychidae	Insect	Filterer	10	LMR1	-28.86±0.17	1.40±0.16
			10	LMR2	-28.77±0.11	1.48±0.64
			5	LMR3	-29.21±0.17	1.67±0.27
			5	LMR4	-27.73±0.20	3.25±0.25
			5	LMR5	-32.74±0.08	3.49±0.08
			5	LMR6	-31.51±0.11	3.05±0.31

			5	LMR7	-30.75±0.20	2.77±0.04
			5	NIO1	-22.92±0.05	3.50±0.28
			5	NIO2	-24.70±0.03	3.05±0.08
			5	NIO3	-27.07±0.04	3.53±0.02
			5	NIO5	-22.89±0.04	3.67±0.09
			5	NIO6	-25.25±0.04	5.03±0.14
			5	NIO7	-27.21±0.11	0.55±0.08
			5	NIO8	-23.28±0.04	6.75±0.14
Isonychiidae	Insect	Filterer	5	LMR1	-29.60±0.80	1.36±0.12
			5	NIO1	-24.70±0.15	4.37±0.11
			5	NIO5	-24.54±0.24	4.15±0.30
			5	NIO8	-25.20±0.19	5.64±0.20
Leptoceridae (nectopsyche)	Insect	Shredder	5	NIO6	-24.90±0.11	5.86±0.20
Leptohyphidae		Collector Gatherer	3	LMR4	-26.16±0.11	1.71±0.32
Leptophlebidae	Insect	Collector Gatherer	5	LMR6	-29.91±0.23	2.60±0.15
			5	LMR7	-31.56±0.07	1.78±0.20
Libeluliidae	Insect	Predator	5	NIO5	-25.15±0.1	2.81±0.12
Naucoridae	Insect	Predator	5	LMR6	-30.35±0.21	3.47±0.13
			3	LMR7	-30.15±0.06	2.66±0.15
			5	NIO5	-24.44±0.07	4.73±0.16
			3	NIO7	-23.66±0.48	4.01±1.16
			5	NIO8	-24.75±0.18	5.42±0.33
Nepidae	Insect	Predator	5	NIO1	-31.73±0.27	3.71±0.55
			5	NIO6	-30.08±0.16	4.44±0.32
Northern Crayfish	Crustacean	Omnivore	5	NIO1	-24.01±0.11	6.00±0.19
			5	NIO6	-24.80±0.04	6.73±0.07
Palaemon	Crustacean	Omnivore	5	NIO8	-22.72±0.26	8.10±0.16
Perlidae	Insect	Predator	10	LMR1	-28.23±0.08	3.18±0.18
			10	LMR2	-28.51±0.10	3.06±0.20
			10	LMR3	-28.10±0.29	3.53±0.15
			6	LMR4	-27.20±0.56	4.85±0.17
			3	NIO1	-24.07±0.07	5.96±0.07
Physidae	Mollusk	scraper	5	LMR5	-28.68±0.05	3.31±0.01
			2	LMR6	-28.06±0.36	2.88±0.11
			5	LMR7	-24.14±0.16	4.63±0.24
			5	NIO1	-21.37±0.37	2.41±0.82
			5	NIO3	-24.81±0.10	5.87±0.18
			5	NIO5	-23.23±0.07	3.85±0.20
			5	NIO8	-20.00±0.21	5.28±0.07

Pterynarcidae	Insect	Shredder	15	NIO1	-24.31±0.12	2.34±0.25
			10	NIO6	-25.82±0.18	4.10±0.49
			6	NIO7	-27.85±0.24	1.54±0.49
			5	NIO8	-24.30±0.03	5.12±0.09
Simuliidae	Insect	Filterer	5	LMR1	-27.90±0.11	1.12±0.11
			5	LMR3	-28.79±0.10	1.56±0.10
			4	LMR4	-27.67±0.16	2.76±0.09
			5	LMR5	-31.64±0.19	3.63±0.05
			5	LMR7	-30.98±0.12	1.51±0.073
			5	NIO3	-24.99±0.06	3.06±0.07
Tipulidae (tipulinae)	Insect	Shredder	5	NIO7	-26.54±0.20	1.03±0.17

Table 6. Community trophic metrics across all sample sites. Community trophic metric descriptions can be found in the methods section, but briefly, CR is carbon range, NR is nitrogen range, TA is total area, CD is mean distance to centroid, MNND is the mean nearest neighbor distance and SDNND is the standard deviation of nearest neighbor distance. All community trophic data is the mean centroid value.

Patch	CR	NR	TA	CD	MNND	SDNND
LMR1	2.049	3.292667	3.485203	1.169105	1.03836	0.54309
LMR2	1.975	4.518	4.708485	1.790155	1.429163	0.132389
LMR3	6.418	2.4	6.036702	2.096305	1.768162	1.713843
LMR4	4.256	6.252	9.514001	1.863333	1.146479	1.51558
LMR5	1.276667	4.063333	3.485114	1.400607	0.941019	0.371323
LMR6	4.848	4.7995	11.104	1.735127	1.392899	1.183449
LMR7	5.67	7.426	19.9124	2.088894	1.3386	1.367119
NIO1	3.746	10.35	22.18286	2.391378	1.155886	0.974021
NIO2	3.714	5.22	7.904103	2.571395	2.044749	2.127764
NIO3	5.034	7.152	17.53281	2.24801	1.276341	0.799173
NIO5	3.006	11.424	13.56566	2.30374	1.216382	1.468102
NIO6	4.08	5.712	14.4799	1.929389	0.725665	0.3309
NIO7	3.536	6.097333	11.03264	1.887082	1.097086	0.75515
NIO8	2.978	5.19	8.098336	1.535558	0.858821	0.950439

Figures

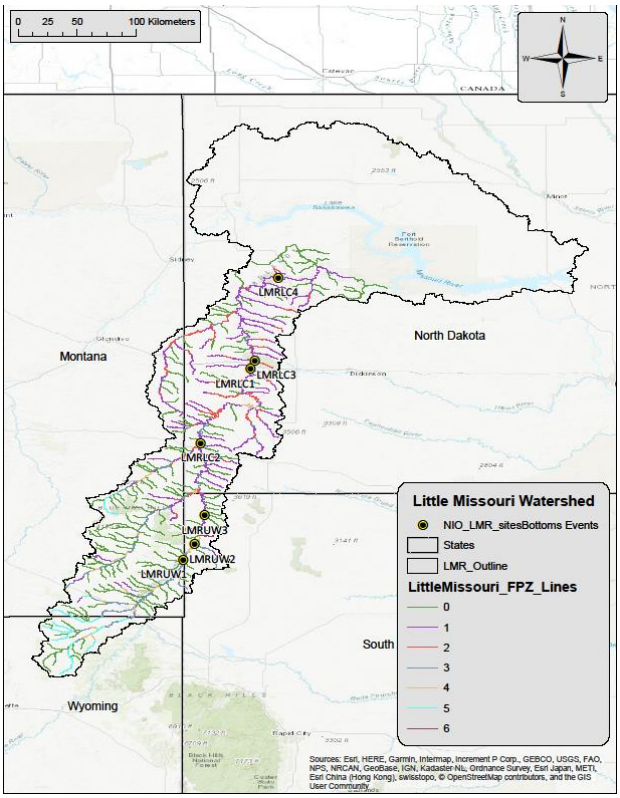

Figure 1. Map of sample sites within the Little Missouri watershed. The sites that were sampled are labeled with the RESonate site code but were changed for my study. LMRLC1=LMR1 and increased in number for all LMRLC sites until LMR4. LMRUW1=LMR5 and increased for the last two sites until LMR7.

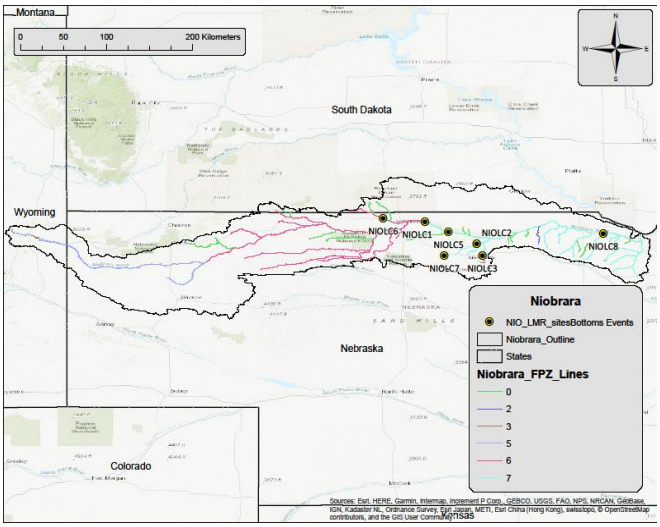

Figure 2. Map of the sties sampled in the Niobrara watershed. Original site codes were based off the RESonate model but were changed for my study, NIOLC1=NIO1 up until NIO8.

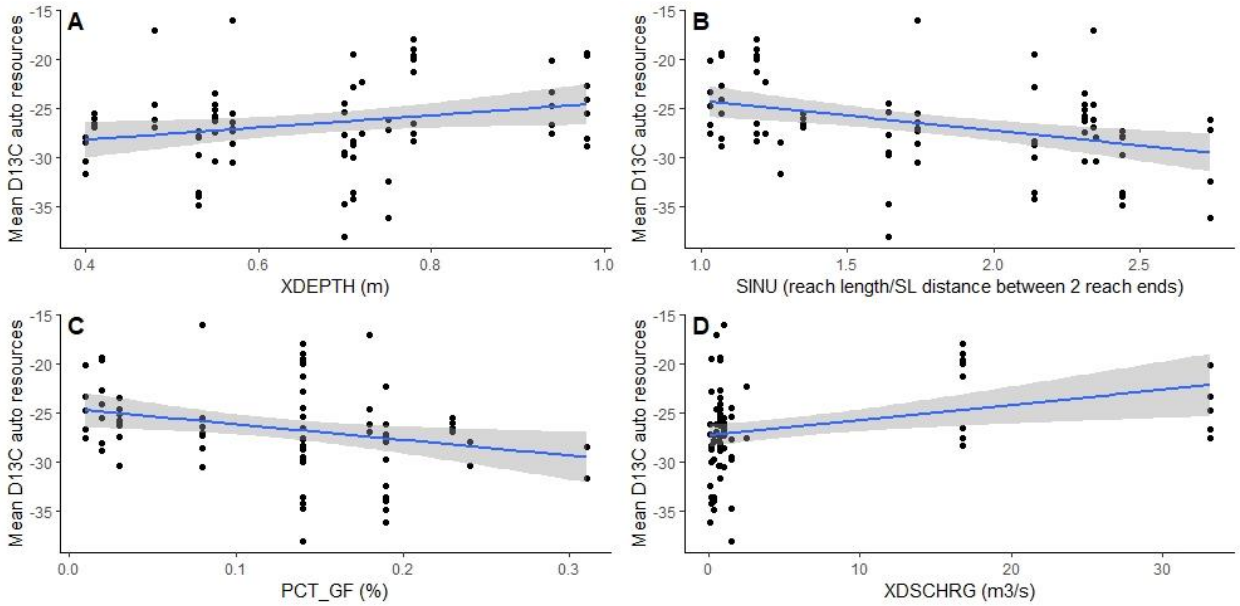

Figure 3. Matrix of scatterplots between the mean $\delta^{13}C$ of autochthonous sources and four different hydrogeomorphic variables. The hydrogeomorphic variables are XDEPTH (A), SINU (B), PCT_GF (C), and XDSCHRG (D). Variable explanations can be found in Table 1. Each point represents the mean $\delta^{13}C$ of a particular autochthonous food source. Autochthonous food sources from all sites except LMR4 were included in each scatterplot. Sinuoisty is measured as the reach length divided by the straight-line distance between 2 reach ends. Plot D is the only plot that does not have a significant relationship after the outliers are removed ($p=0.062$, $R^2=11.1\%$). The other relations are all significant: XDEPTH ($p=0.013$, $R^2=14.0\%$), SINU ($p=0$, $R^2=32.1\%$) and PCT_GF ($p=0.013$, $R^2=14.8\%$).

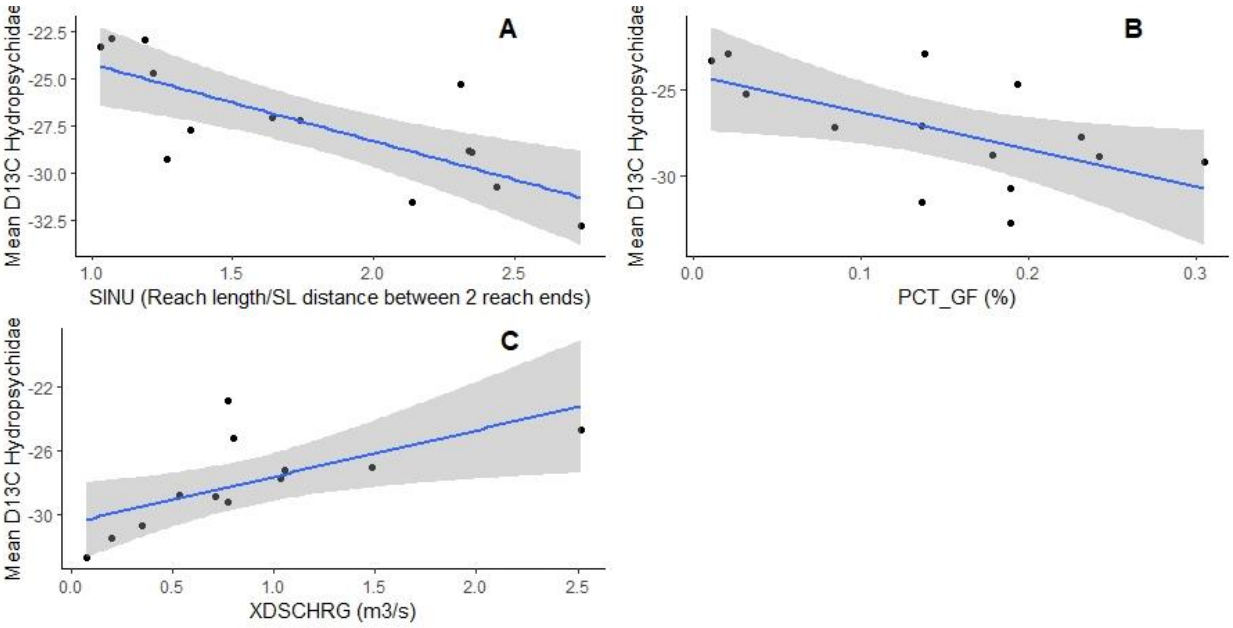

Figure 4. Matrix of scatterplots between the mean $\delta^{13}C$ of Hydropsychidae and three different hydrogeomorphic variables from each site. The hydrogeomorphic variables are: SINU (A), PCT_GF (B), XDSCHRG (C). Variable explanations can be found in Table 1. Each point represents the mean $\delta^{13}C$ of Hydropsychidae from a specific site, totaling 12 points. Sinuoisty is measured as the reach length divided by the straight-line distance between 2 reach ends. All relations are statistically significant: SINU (p=0.002, R^2=56.4%), PT_GF (p=0.028, R^2=34.1%) and XDSCHRG (p=0.02, R^2=43.1) excluding the two outliers from sites NIO8 and NIO1, so only 10 points are included in (C).

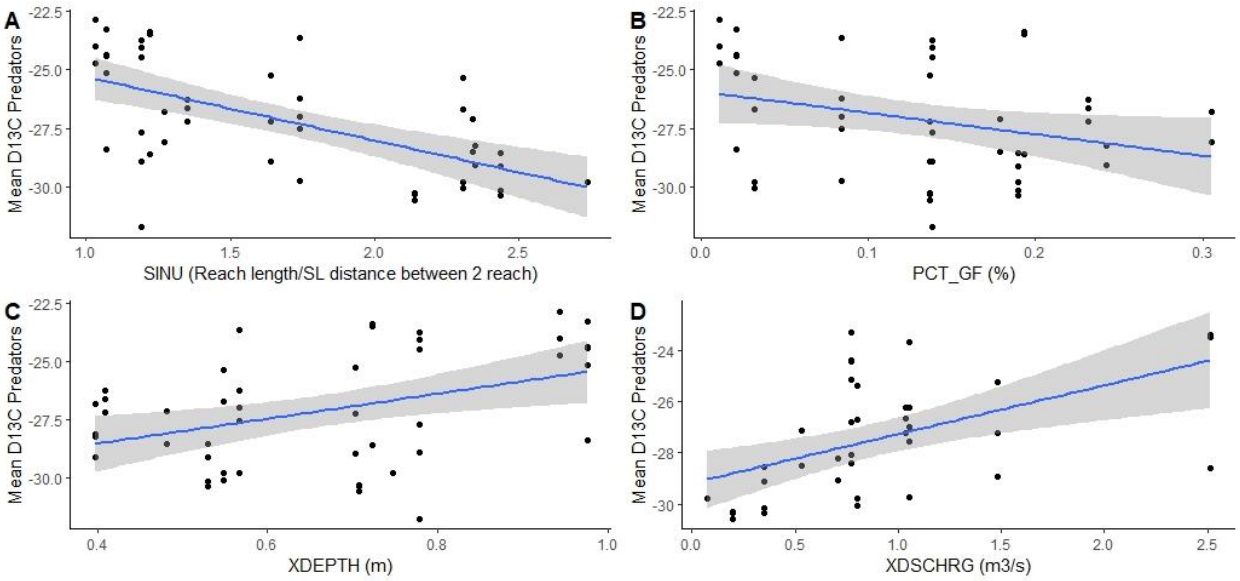

Figure 5. Matrix of scatterplots between the mean $\delta^{13}C$ of predators to four hydrogeomorphic variables. The four hydrogeomorphic variables are: SINU (A), PCT_GF (B), XDEPTH (C), and XDSCHRG (D). Variable explanations can be found in Table 1. Each point represents the mean $\delta^{13}C$ of a specific predator from each site. Sinuosity is measured as the reach length divided by the straight-line distance between 2 reach ends. Each relationship is significant: SINU (p=0, R^2=36.2%), PCT_GF (p=0.038, R^2=9.4%), XDEPTH (p=0.005, R^2=16.3%) and XDSCHRG without outliers (p=0.001, R^2=26.1%).

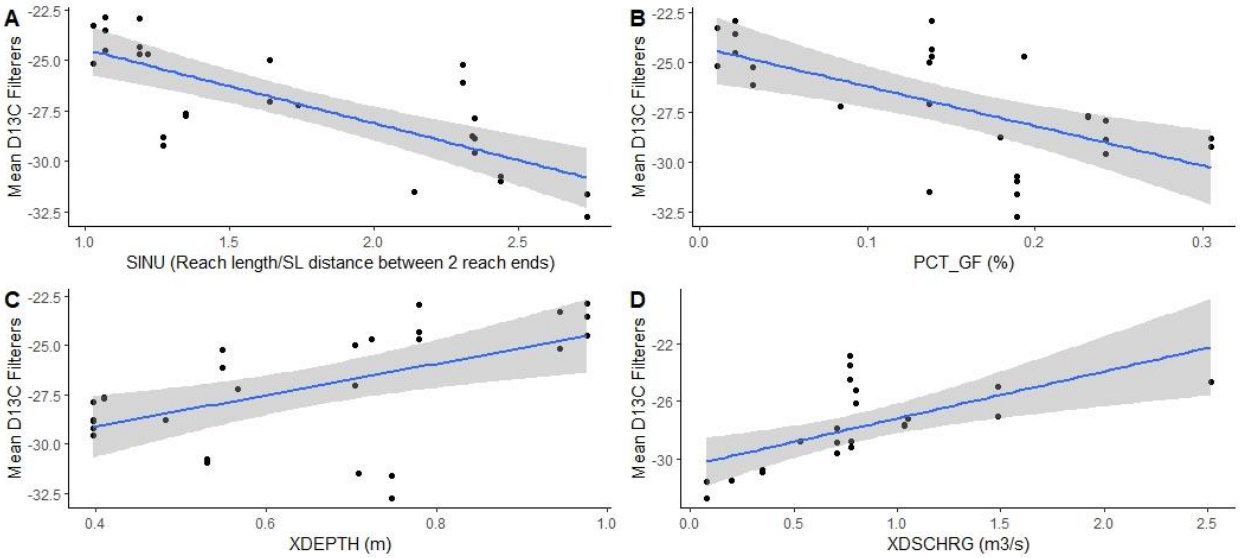

Figure 6. Matrix of scatterplots between the mean $\delta^{13}C$ of filterers from each site to four hydrogeomorphic variables. The hydrogeomorphic variables are: SINU (A), PCT_GF (B), XDEPTH (C) and XDSCHRG without outliers from NIO8 & 1 (D). Variable explanations can be found in Table 1. Each point represents the mean $\delta^{13}C$ of a specific filter feeder from a specific site. All relationships are significant: SINU (p=0, R^2=57.8%), PCT_GF (p=0.001, R^2=38.9%), XDEPTH (p=0.002, R^2=31.4%) and XDSCHRG (p=0.002, R^2= 39.8%).

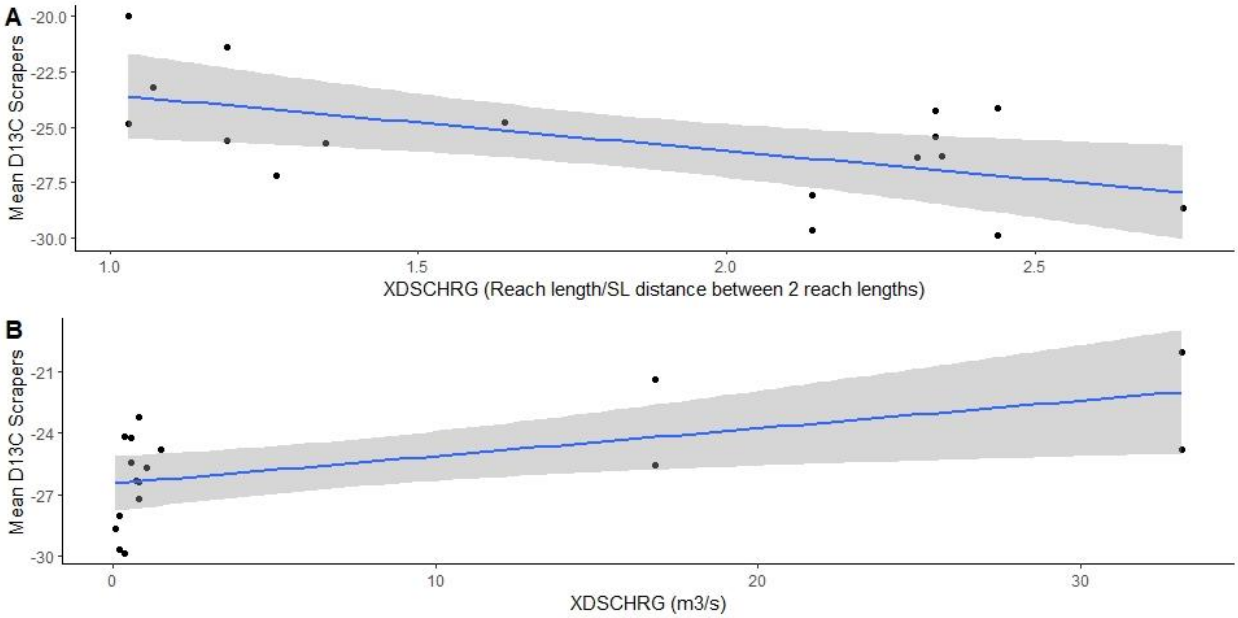

Figure 7. Matrix of scatterplots between two different hydrogeomorphic variables and the mean $\delta^{13}C$ of scrapers. The hydrogeomorphic variables are SINU (A) and XDSCHRG (B). Variable explanations can be found in Table 1. Each point represents the mean $\delta^{13}C$ of a scraper from a particular site. All sites were included except NIO2 and NIO7 where no scrapers were collected. Sinuosity was significant ($p=0.014$, $R^2=33.9\%$) and XDSCHRG was not when the two outliers were excluded ($p=0.057$, $R^2=29.1\%$).

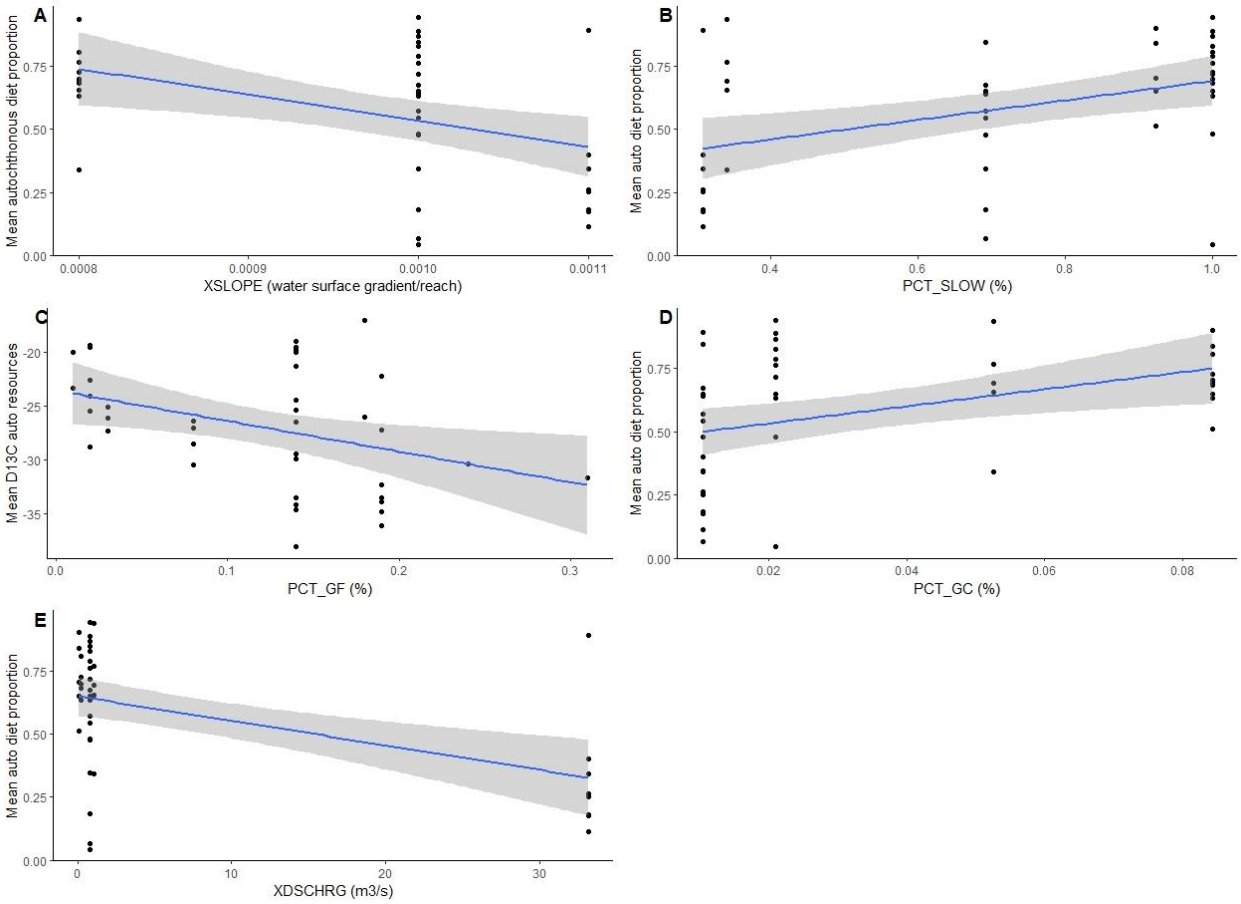

Figure 8. Matrix of scatterplots between three hydrogeomorphic variables against the mean autochthonous diet proportion of consumers. The three different hydrogeomorphic variables were: XSLOPE (A), PCT_SLOW (B), PCT_GC (C), PCT_GF (D) and XDSCHRG (E). Variable explanations can be found in Table 1. Each point represents the mean diet proportion of a specific consumer from a particular site. Sites included in analysis are: LMR5, LMR6, NIO5, NIO6, NIO7, NIO8. All relationships were significant: XSLOPE ($p=0.005$, $R^2=18.7\%$), PCT_SLOW ($p=0.003$, $R^2=19.2\%$), PCT_GC ($p=0.007$, R2=15.74%), PCT_GF with an outlier removed (0.043, R2=10.3), except for XDSCHRG when the two outliers were excluded ($p=0.303$, $R^2=3.1\%$).

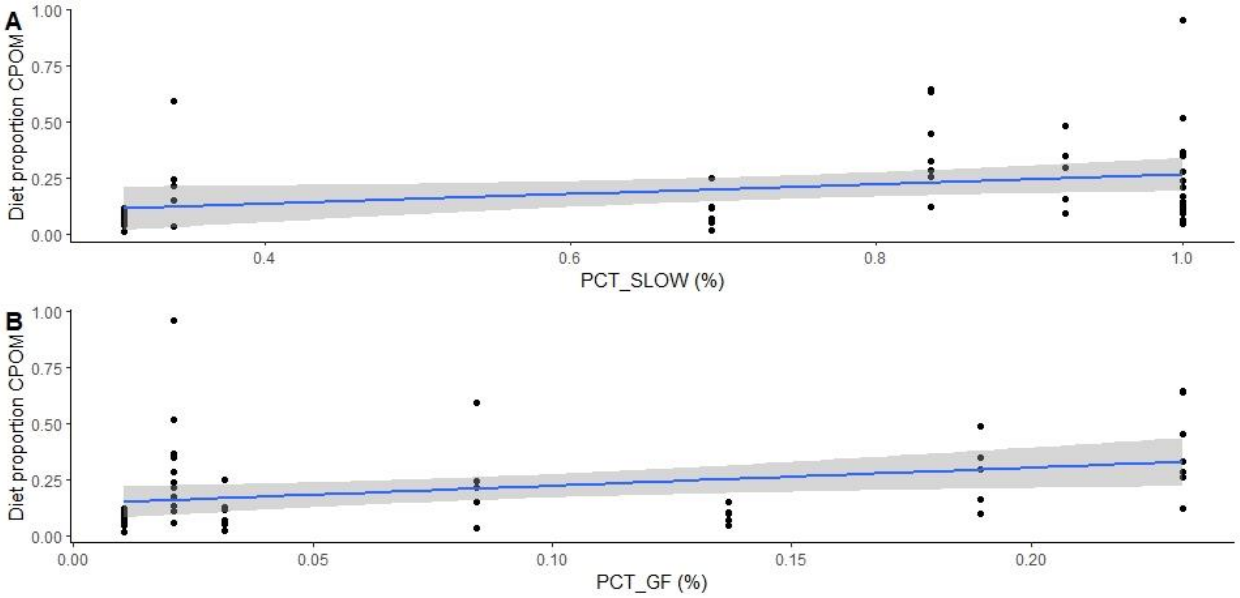

Figure 9. Matrix of scatterplots analyzing the relationships between two hydrogeomorphic variables and the mean CPOM diet proportion of consumers. The two hydrogeomorphic variables were PCT_SLOW (A) and PCT_GF (B). Sites included in analysis are: LMR4, LMR5, LMR6, NIO5, NIO6, NIO7, NIO8. Variable explanations can be found in Table 1. Each point represents the mean CPOM diet proportion of a particular consumer from a particular site. Both relationships were significant with PCT_SLOW (p=0.028, R^2=9.3%) and PCT_GF (0.014, R^2=11.4%).

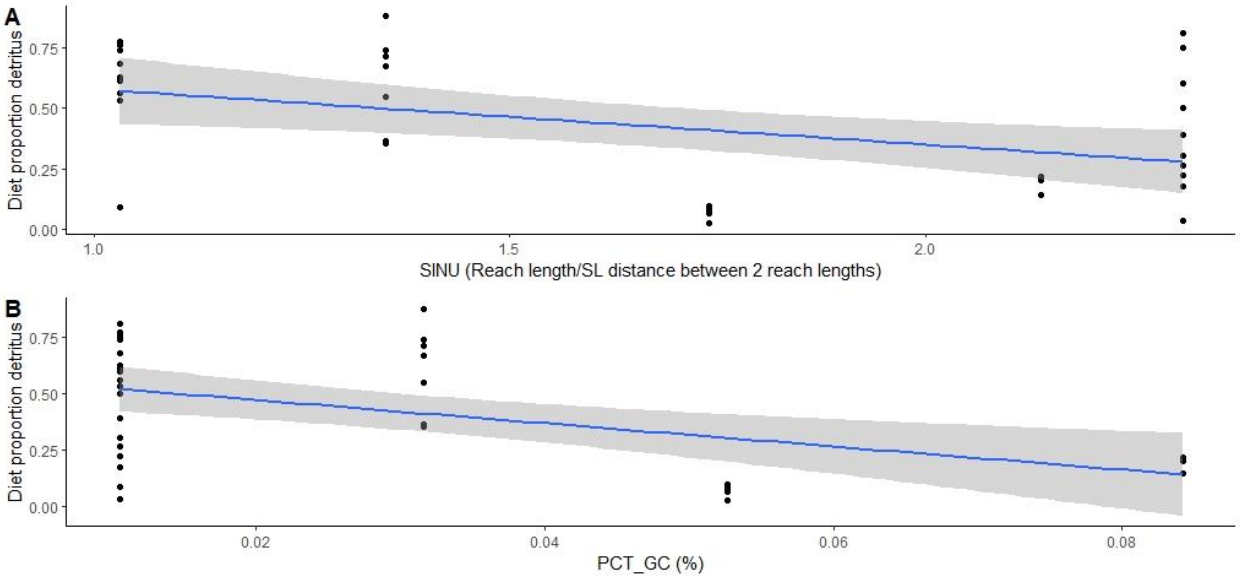

Figure 10. Matrix of scatterplots analyzing the relationships between the two different hydrogeomorphic variables and the mean detrital diet proportion of all consumers. The two hydrogeomorphic variables were SINU (A) and PCT_GC (B). Variable explanations can be found in Table 1. Sites included in analysis are: LMR4, LMR6, NIO6, NIO7 and NIO8. Each point represents the mean detrital proportion of a particular consumer from a specific site. Both relationships were significant with SINU (p=0.007, R^2=19.7%) and PCT_GC (0.002, R^2=25.4).

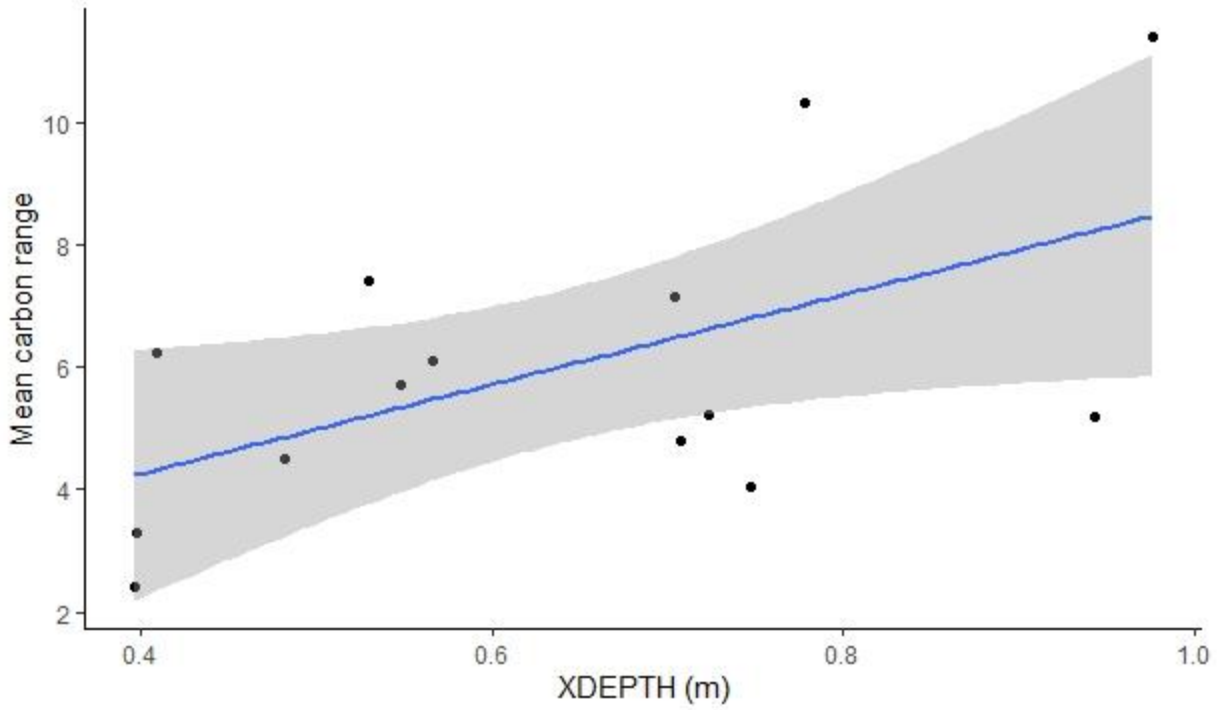

Figure 11. Scatterplot of the statistically significant relationship (p=0.037, R^2=31.5%) between (XDEPTH) mean thalweg depth and the carbon range community metric. Each point represents the carbon range for a specific community, for a total of 14 points.

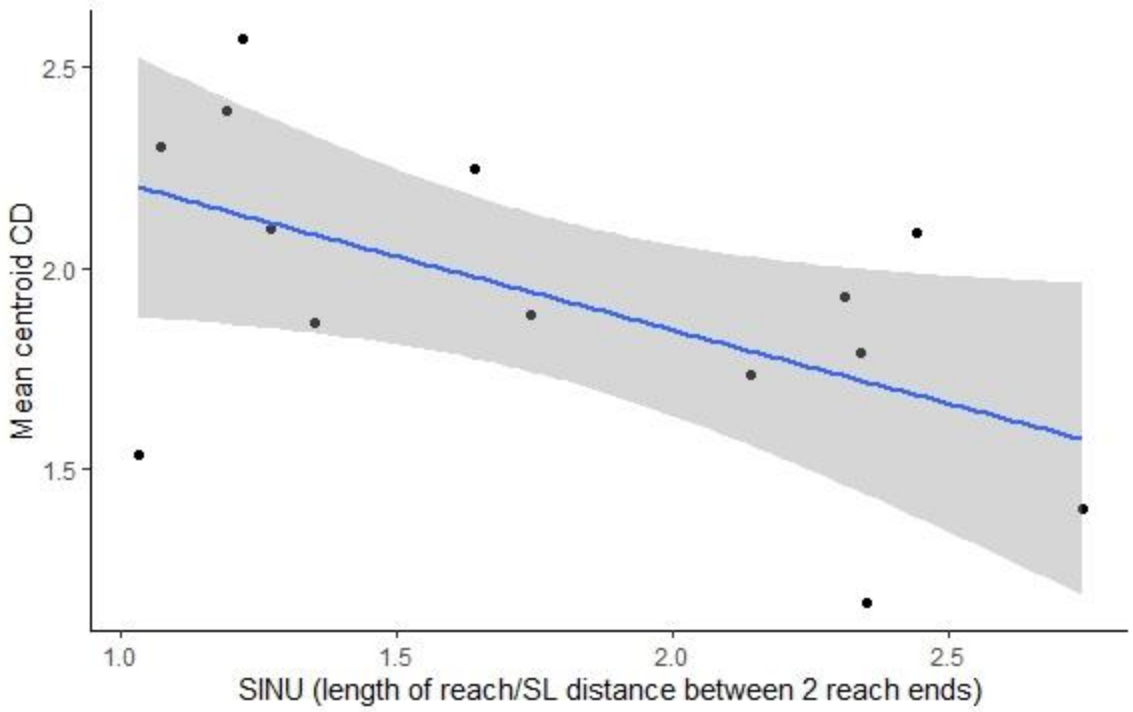

Figure 12. Scatterplot of the significant relationship between the mean centroid CD and sinuosity (SINU) (p=0.038, R^2=31.1%). Each point represents the mean CD of a specific community, for a total of 14.

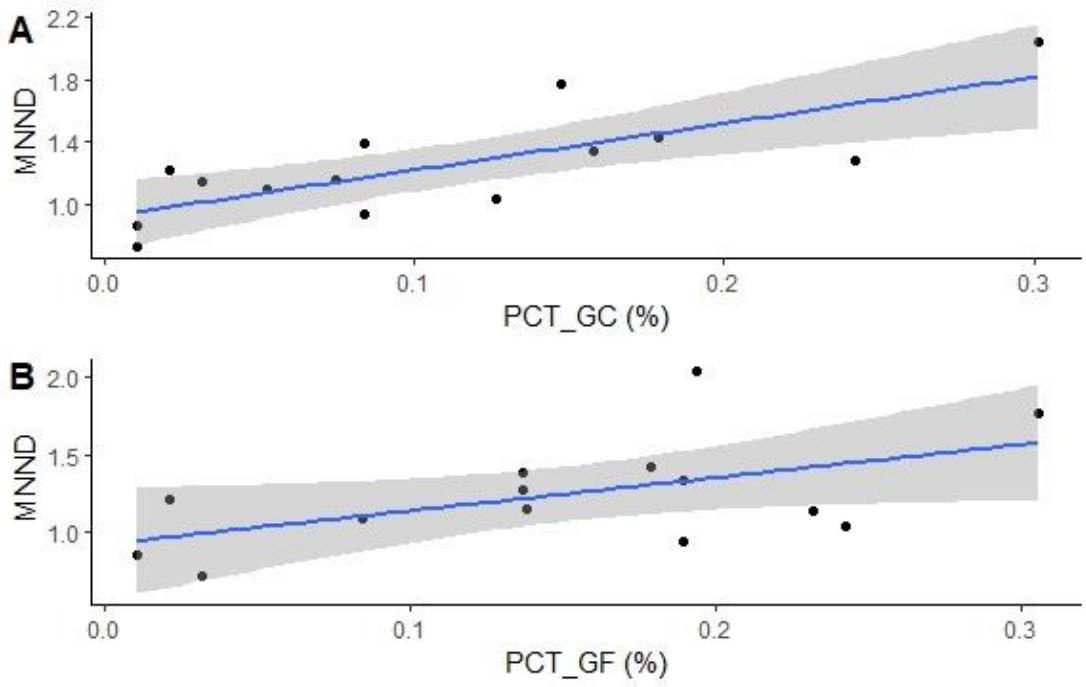

Figure 13. Scatterplot of the relationship between two hydrogeomorphic variables and MNND. The two hydrogeomorphic variables were PCT_GC (A) and PCT_GF (B). Variable explanations can be found in Table 1. Both of the relationships are statistically significant: ($p=0.001$, $R^2=58.3\%$) and ($p=0.047$, $R^2=29\%$) consecutively. Each point represents MNND from a specific site for a total of 14.

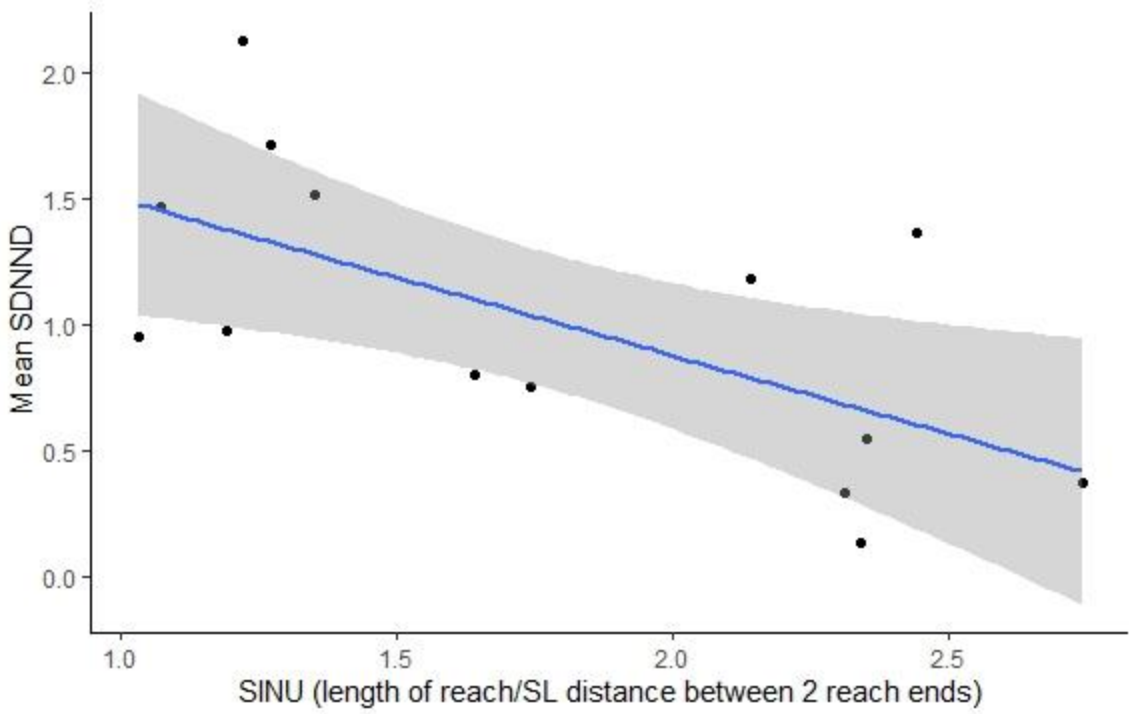

Figure 14. Scatterplot of the significant relationship between SDNND and sinuosity (SINU) ($p=0.013$, $R^2=41.1\%$). The points represent a specific SDNND measurement from a specific site for a total of 14 sites. SL in the x axis stands for straight line.

References

Allan, J., D, & Catillo, M., M. (2007). *Stream Ecology: Structure and function of running waters*. The Netherlands: Springer.

Atkinson, B. L., Grace, M. R., Hart, B. T., & Vanderkruk, K. E. (2008). Sediment instability affects the rate and location of primary production and respiration in a sand-bed stream. *Journal of the North American Benthological Society, 27*(3), 581-592.

Bellamy, A. R., Bauer, J. E., & Grottoli, A. G. (2017). Influence of land use and lithology on sources and ages of nutritional resources for stream macroinvertebrates: a multi-isotopic approach. *Aquatic Sciences, 79*(4), 925-939. doi:10.1007/s00027-017-0542-3

Cremona, F., Hamelin, S., Planas, D., & Lucotte, M. (2009). Sources of organic matter and methylmercury in littoral macroinvertebrates: a stable isotope approach. *Biogeochemistry, 94*(1), 81-94.

Dodds, W. K., Gido, K., Whiles, M. R., Fritz, K. M., & Matthews, W. J. (2004). Life on the edge: the ecology of Great Plains prairie streams. *BioScience, 54*(3), 205-216.

Finlay, J. C. (2004). Patterns and controls of lotic algal stable carbon isotope ratios. *Limnology and Oceanography, 49*(3), 850-861.

Gannes, L., Z.,, Martı´nez del Rio, C., & Koch, P. (1998). Natural abundance variations in stable isotopes and their potential uses in animal physiological ecology. *Comparative Biochemistry and Physiology, 119*(3), 725-737.

Hamilton, S., K, Sippel, S., J, & Bunn, S., E. (2005). Separation of algae from detritus for stable isotope or ecological stoichiometry studies using density fractionation in colloidal silica. *Limnology and Oceanography: Methods, 3*, 149-157.

Ishikawa, N. F., Doi, H., & Finlay, J. C. (2012). Global meta-analysis for controlling factors on carbon stable isotope ratios of lotic periphyton. *Oecologia, 170*(2), 541-549.

Jackson, A. L., Inger, R., Parnell, A. C., & Bearhop, S. (2011). Comparing isotopic niche widths among and within communities: SIBER–Stable Isotope Bayesian Ellipses in R. *Journal of Animal Ecology, 80*(3), 595-602.

Jardine, J., D, Curry, A., R, Heard, K., S, & Cunjak, R., A. (2005). High fidelity: isotopic relationship between stream invertebrates and their gut contents. *North American Benthological Society, 24*(2), 290-299.

Kaehler, S., & Pakhomov, E., A. (2001). Effects of storage and preservation on the 13C and 15N signatures of selected marine organisms. *Marine Ecology Progress Series, 219*, 299-304.

Kobayashi, S., Akamatsu, F., Amano, K., Nakanishi, S., & Oshima, Y. (2011). Longitudinal changes in δ13C of riffle macroinvertebrates from mountain to lowland sections of a gravel-bed river. *Freshwater Biology, 56*(7), 1434-1446.

Layman, C. A., Arrington, D. A., Montaña, C. G., & Post, D. M. (2007). Can stable isotope ratios provide for community-wide measures of trophic structure? *Ecology, 88*(1), 42-48.

Matthews, W. J. (1988). North American prairie streams as systems for ecological study. *Journal of the North American Benthological Society, 7*(4), 387-409.

McConnaughey, T. A., & Gillikin, D. P. (2008). Carbon isotopes in mollusk shell carbonates. *Geo-Marine Letters, 28*(5-6), 287-299.

Newsome, S. D., Martinez del Rio, C., Bearhop, S., & Phillips, D. L. (2007). A niche for isotopic ecology. *Frontiers in Ecology and the Environment, 5*(8), 429-436.

Poole, G. C. (2010). Stream hydrogeomorphology as a physical science basis for advances in stream ecology. *Journal of the North American Benthological Society, 29*(1), 12-25.

Post, D. M. (2002). Using stable isotopes to estimate trophic position: models, methods, and assumptions. *Ecology, 83*(3), 703-718.

R Development Core Team. (2018). RStudio: Integrated Development for R. Boston, Massachusetts: RStudio, Inc. Retrieved from http://www.rstudio.com/

Rasmussen, J. B., & Trudeau, V. (2010). How well are velocity effects onð 13C signatures transmitted up the food web from algae to fish? *Freshwater Biology, 55*(6), 1303-1314.

Schmidt, S. N., Vander Zanden, M. J., & Kitchell, J. F. (2009). Long-term food web change in Lake Superior. *Canadian Journal of Fisheries and Aquatic Sciences, 66*(12), 2118-2129.

Smith, J. A., Mazumder, D., Suthers, I. M., Taylor, M. D., & Bowen, G. (2013). To fit or not to fit: evaluating stable isotope mixing models using simulated mixing polygons. *Methods in Ecology and Evolution, 4*(7), 612-618. doi:10.1111/2041-210x.12048

Smits, A. P., Schindler, D. E., & Brett, M. T. (2015). Geomorphology controls the trophic base of stream food webs in a boreal watershed. *Ecology, 96*(7), 1775-1782.

Stock, B. C., Jackson, A. L., Ward, E. J., Parnell, A. C., Phillips, D. L., & Semmens, B. X. (2018). Analyzing mixing systems using a new generation of Bayesian tracer mixing models. *PeerJ, 6*, e5096. doi:10.7717/peerj.5096

Sullivan, S. M. P. (2013). Stream foodweb δ13C and geomorphology are tightly coupled in mountain drainages of northern Idaho. *Freshwater Science, 32*(2), 606-621. doi:10.1899/12-101.1

Thoms, M. C., Delong, M. D., Flotemersch, J., E., & Collins, S., E. (2017). Physical heterogeneity and aquatic community function in river networks: A case study from the Kanawha River Basin, USA. *Geomorphology, 290*, 277-287.

Thorp, J. H., Thoms, M. C., & Delong, M. D. (2006). The riverine ecosystem synthesis: biocomplexity in river networks across space and time. *River Research and Applications, 22*(2), 123-147. doi:10.1002/rra.901

Thorp, J. H., & Rogers, D. C. (2015). *Thorp and Covich's Freshwater Invertebrates: Keys to Nearctic Fauna* (4 ed.): Elsevier Science.

Vannote, R. L., Minshall, G. W., Cummins, K. W., Sedell, J. R., & Cushing, C. E. (1980). The River Continuum Concept. *Canadian Journal of Fisheries and Aquatic Sciences, 37*, 130-137.

Williams, B. S., D'Amico, E., Kastens, J. H., Thorp, J. H., Flotemersch, J. E., & Thoms, M. C. (2013). Automated riverine landscape characterization: GIS-based tools for watershed-scale research, assessment, and management. *Environmental monitoring and assessment, 185*(9), 7485-7499.

Zambrano, L., Valiente, E., & Vander Zanden, M. J. (2010). Food web overlap among native axolotl (Ambystoma mexicanum) and two exotic fishes: carp (Cyprinus carpio) and tilapia (Oreochromis niloticus) in Xochimilco, Mexico City. *Biological Invasions, 12*(9), 3061-3069.